DNA Nanotechnology Hot Paper

How to cite:
International Edition: doi.org/10.1002/anie.202006384
German Edition: doi.org/10.1002/ange.202006384

Cut and Paste for Cancer Treatment: A DNA Nanodevice that Cuts Out an RNA Marker Sequence to Activate a Therapeutic Function

*Tatiana A. Molden, Caitlyn T. Niccum, and Dmitry M. Kolpashchikov**

Abstract: *DNA nanotechnology uses oligonucleotide strands to assemble molecular structures capable of performing useful operations. Here, we assembled a multifunctional prototype DNA nanodevice, DOCTR, that recognizes a single nucleotide mutation in a cancer marker RNA. The nanodevice then cuts out a signature sequence and uses it as an activator for a "therapeutic" function, namely, the cleavage of another RNA sequence. The proposed design is a prototype for a gene therapy DNA machine that cleaves a housekeeping gene only in the presence of a cancer-causing point mutation and suppresses cancer cells exclusively with minimal side effects to normal cells.*

Introduction

Programmable and autonomous computing machine made of biomolecules can become a tool for manipulating nature at the molecular and atomic levels and thus help controlling both human health and materials' properties.[1] DNA nanotechnology deals with assembling a broad variety of functional molecular structures including DNA machines.[2] Recently, DNA associations capable of intracellular detection of cancer markers,[3–5] and delivery of therapeutic payloads inside cells[6–8] have been designed. We undertake a seemingly logical step of applying DNA nanotechnology to improve oligonucleotide gene therapy (OGT). Conventional OGT agents include antisense, siRNA, CRISPR/cas9 and deoxyribozymes (Dz).[9,10] However, none of them has produced a clinically significant anti-cancer treatment so far. Indeed, among the 6 anti-cancer gene therapy drugs approved by August 2019, there is not a single OGT.[11] We believe that sophisticated oligonucleotide-based nanodevices can be more effective in anticancer treatment than traditional OGT agents. In our definition, therapeutic oligonucleotide nanodevices are multifunctional nanoconstructs, which at a minimum must include the following functionalities: ability to recognize an aberrant signal, process it, and take an action, such as destruction of a molecule or a cell.[12] DNA nanodevices containing a built-in "processor" capable of analyzing the signals can be called "DNA nanorobots".[12] Our long term goal is to design a DNA nanorobot that can (i) penetrate into cytoplasm of a targeted cell; (ii) analyze a complex pattern of cancer markers to ensure high selectivity of cancer cell recognition; (iii) autonomously activate its cleaving function upon target recognition; (iv) be able to unwind an RNA target secondary and tertiary structure; (v) cleave multiple copies of a vital (presumably housekeeping gene) RNA target. One advantage of such approach in comparison with traditional OGT agents, is cancer cells-specific activation thus eliminating a risk of damaging healthy cells.[13] Another advantage, is the possibility to target mRNAs of the genes other than cancer markers, which should increase efficiency of cancer cell suppression.[14] We previously described a nanodevice, that would target mRNA vital for cell survival upon activation by cancer marker,[14] with the goal to trigger cancer cell death. In intracellular environment, however, a cancer marker-bound nanorobots can lose their intracellular mobilities required for finding RNA targets. In this paper, we describe a DNA nanodevice that recognizes an RNA cancer marker with high selectivity, cuts a short fragment from the context of longer RNA sequence, which is followed by cleaving a housekeeping gene mRNA. We achieved single nucleotide selectivity of marker RNA recognition under near physiological conditions.

Results and Discussion

The principle of the DNA nanodevice, named here "the Deoxyribozyme-Operated Cancer-Targeting nanoRobot" (DOCTR), is shown in Figure 1A. The construct is based on an RNA-cleaving deoxyribozyme (Dz)—short DNA that can cleave specific RNA sequences.[15] It consists of the two cancer marker-cleaving Dz (Dz1 and Dz2) and strands Dz-a and Dz-b, attached to a double-stranded (ds) DNA platform (Figure 1A). DOCTR-1 recognizes a fragment of a cancer marker RNA characterized by a single base cancer-causing mutation. This leads to cutting out short activating fragment (bold in Figure 1A), which "bridges" Dz-a and Dz-b fragments of DOCTR-1. It is speculated that the now "active" DOCTR can freely migrate inside the cell searching for its cognate mRNA targets. Brought together, Dz-a and Dz-b reform a Dz catalytic core that cleaves a targeted RNA (e.g. a housekeeping gene mRNA). Cleavage of mRNA target will trigger cancer cell death.

As a cancer marker, we chose the KRAS gene mRNA. Ras proteins, encoded by HRAS, NRAS and KRAS genes, are GTPases involved in cellular growth and proliferation.[16] Mutation hotspots at codons 12, 31, and 61 have been found in ≈25% of all human cancers.[16] Moreover, about 87% of all Ras mutations occur within KRAS isoform almost exclusively at codon 12, where G→A nucleotide substitution is the most

[*] T. A. Molden, C. T. Niccum, Dr. D. M. Kolpashchikov
Chemistry Department, University of Central Florida
Orlando, FL 32816 (USA)
E-mail: dmitry.kolpashchikov@ucf.edu

Supporting information and the ORCID identification number(s) for the author(s) of this article can be found under: https://doi.org/10.1002/anie.202006384.

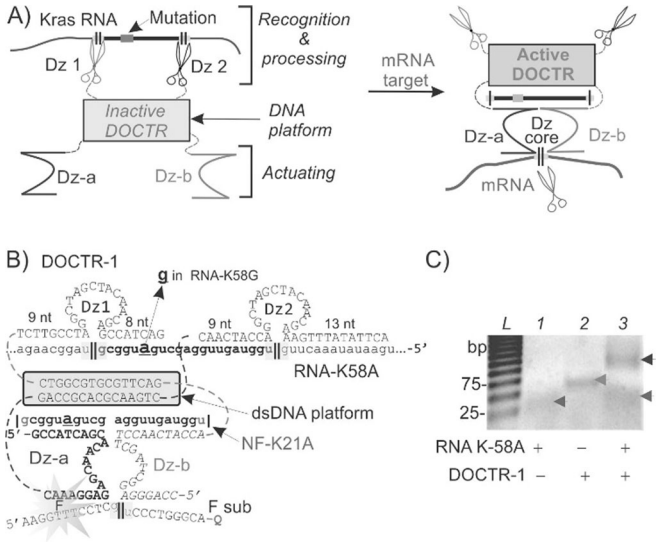

Figure 1. Design and assembly of Deoxyribozyme-Operated Cancer-Targeting nanoRobot (DOCTR). A) Principle design: DOCTR cuts out a fragment of an RNA cancer marker (bold) after which it activates cleavage of the mRNA target. | | indicates cleavage sites. B) DOCTR-1 cuts out a 21-nt fragment (NF-21A) from K58A RNA. Shaded region represents the dsDNA platform. Dashed lines are triethylene glycol linkers. The g > a mutation differentiates cancer marker K58A from normal K58G. Dz-a and Dz-b form the active Dz core after binding NF-21A followed by cleavage of a fluorogenic substrate (F sub). C) Analysis of DOCTR-1 assembly by agarose gel electrophoresis. Lanes 1 and 2 contained K58A and DOCTR-1. Lane 3 contained a mixture of 42 nM DOCTR-1 and 420 nM RNA K58A. Arrows indicate positions of the K58A, DOCTR-1, and DOCTR-1/K58A complexes. Lane L contains a double-stranded (ds) DNA ladder indicated in base pairs (bp).

common.[12] Mutations in Kras has been previously targeted using Dz 10–23[17] and siRNA technologies.[18] However, despite significant efforts in targeting Kras, no clinically significant therapy has been reported to date. Kras was dubbed an "undruggable target" due to retention of cancer cell viability even after Kras was knocked down.[19] In this study, DOCTR-1 was designed to recognize the G→A nucleotide substitution followed by cleaving of a vital housekeeping gene thus providing a principle solution of the "undruggability" problem. We used synthetic RNA K58G as a marker of healthy cells, and mutated RNA K58A as a marker of cancer cells (Figure 1B and Table S1).

DOCTR-1's recognition/processing function was carried out by Dz1 and Dz2 (in Figure 1B), both of which a based on Dz10-23 core.[20] The actuating function was carried out by the split Dz[21] consisting of Dz-a and Dz-b fragments. In the absence of RNA cancer marker, the actuating function was inactive. In the presence of a 21-nt fragment (NF-21) of the mutated RNA K58A, Dz-a and Dz-b were brought together, thus forming Dz 10–23 catalytic core to enable the actuating function. We initially tested the actuating function by fluorescence, where Dz-a and Dz-b cleaved a fluorophore- and quencher-labeled F sub (Figure 1B), and then tailored DOCTR-1 to cleave a fragment of a housekeeping gene.

Figure 1C demonstrates formation DOCTR-1 complex with a mobility of ≈75 bp/150 nucleotides (nt) in agreement with the predicted size of 151 nt (Figure 1C, line 2). The position of the band was sifted up in the presence of K-58A RNA due to the formation of 209 nt DOCTR-1/ K-58A RNA complex (Figure 1C, lane 3).

The objective of the next stage was to achieve selective release of NF-21 (Figure 1B) from the cancer marker K-58A, but not from normal K-58G. All RNA cleaving experiments were performed at 37 °C in the buffer containing 2 mM [Mg^{2+}] to mimic intracellular conditions, in which RNA K-58A folds in a stable secondary structure (Figure S1). We compared several DOCTR constructs in their ability to selectively cleave K-58A, but not K-58G (Figure S2). DOCTR-1 was equipped with Dz1 containing 9-nt and 8-nt RNA-binding arms (Dz1 9/8), and Dz2 with 9-nt and 13-nt RNA-binding arms (Dz2 9/13, see Table S2 for the melting temperatures). The cleavage efficiency of DOCTR-1 was compared with that of the tile-free Dz1 and Dz2 using fluorescein-labeled K-58A-FAM as a substrate. Dz1 produced a 40-nt fluorescent fragment (F-40) and an 18-nt non-fluorescent fragment (NF-18); Dz-2 produced a 19-nt fluorescent fragment (F-19) and a 39-nt non-fluorescent fragment (NF-39). Cleavage of K-58A-FAM by both Dz1 and Dz2 would produce NF-18, F-19, and NF-21 activator sequence (Figure 1B and S1A).

NF-21 was selectively cut out only by DOCTR-1, but not by the detached pair of Dz1 and Dz2. Indeed, DOCTR-1 produced NF-21 when was incubated with cancer marker K-58A, (Figure 2, lane 2). NF-21 fragment was not observed when DOCTR-1 was incubated with normal K-58G RNA (Figure 2, lane 6) suggesting the lack of DOCTR1 activation in healthy cells (Figure 1A and B). This can be explained by the inability of Dz2 to bind K-58G when Dz1/K-58G complex is mismatched. This suggests cooperativity between Dz1 and Dz2 in binding folded RNA. The ability of DOCTR-1 to recognize the least destabilizing G-T mismatch under near physiological conditions is notable. At the same time, tile detached Dz1 and Dz2 of the same sequences (Dz1 9/8 and Dz2 9/13) failed to produce NF-21 fragment (Figure 2, lanes 3

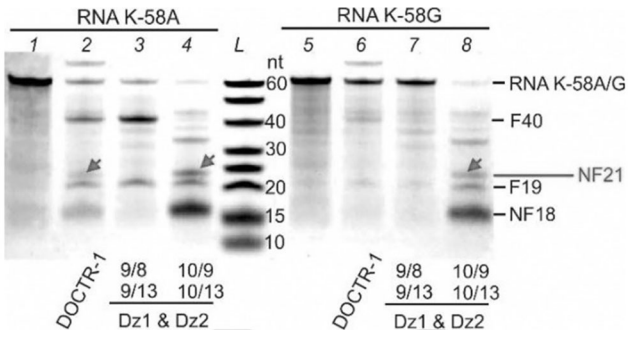

Figure 2. Selectivity of K-58A cleavage by DOCTR-1. All samples contained either 500 nM RNA K-58A (lanes 1–4) or 500 nM K-58G (lanes 5–8). Lanes 1 and 5 contained only RNA K-58A or K-58G as negative controls. Lanes 2–4, 3–8 contained 10 nM of the cleaving agents (DOCTR-1 or Dz) as indicated. All samples were incubated 20 h at 37 °C in buffer 1 (50 mM HEPES, 15 mM NaCl, 150 mM KCl, 2 mM MgCl2, pH 7.4) followed by separation in 12.5% urea polyacrylamide gel. The images were taken under UV light after GelRed staining. Lane L had a single-stranded (ss) DNA ladder indicated in nucleotides (nt). The position of a 21-nt NF-21 activating fragment is indicated by the arrows.

and 7). This can be explained by the combination of the greater cleavage activity of Dz2 with the dimerization of Dz2 cleavage product, NF39 (see discussion to Figure S1).

To achieve NF-21 release by tile-detached Dzs, we tested a series of Dz1 and Dz2 pairs with longer RNA-binding arms (Figure S3). Dz1 10/9 and Dz2 10/13 acting together were able to cut out NF-21 with high efficiency (Figure 2, lane 4). However, they also cut out the same fragment from the wild type K-58G, thus compromising selectivity, so crucial for cancer-specific recognition.

DOCTR-1 cleavage efficiency was, however, lower ($3.8\ h^{-1}$) than that of the tile-free Dz1 and Dz2 ($6.1\ h^{-1}$) under multiple turnover conditions. DOCTR-1's variation lacking Dz-a and Dz-b (DOCTR-2) had cleavage efficiency like that of the tile detached Dz1 and Dz2 pair (Figure S4). This suggests inhibition of the Dz1/Dz2 by the actuating function. Further optimization of DOCTR's structure is required to minimize interference of Dz-a and Dz-b to the processing function.

RNA-58 should initially bind Dz1 and Dz2 due to more favorable binding (sum of ΔG for 4 binding arms is $-32.8\ kcal\,mol^{-1}$) than to Dz-a and Dz-b (sum of ΔG of 2 binding arms is $-26.7\ kcal\,mol^{-1}$). However, after NF-21 activator sequence is cut out, its binding to Dz1 and Dz2 remains weak, causing the NF-21 fragment to be transferred to Dz-a and Dz-b. Nearest neighbor modelling predicts at least $6.2\ kcal\,mol^{-1}$ tighter binding of NF-21 to Dz-a and Dz-b than to Dz-1 and Dz-2 under the experimental conditions. The transfer of the NF-21 fragment to Dz-a and Dz-b should be facilitated by its proximity to the Dz-1 and Dz-2 within DOCTR nanostructure. We hypothesized that the transfer of the NF-21 fragment occurred without its released in solution.

To test this hypothesis, DOCTR-1 was pre-incubated 2 h with K-58A-FAM RNA followed by addition of RNA NF-21-Alexa, a red dye-labeled NF-21 fragment (Table S1). If NF-21 were released in solution after K-58A-FAM processing, NF-21-Alexa would (at least partially) replace NF-21 in the complex with DOCTR-1 thus labeling it red. If there was no exchange, DOCTR-1 would remain unlabeled. Indeed, there was no labeling of DOCTR-1 observed in this sample (Figure 3A, lane 6, upper part). At the same time, RNA K-58A was processed by DOCTR-1, as evident by the release of F-19 product (arrows in lines 4 and 6). The DOCTR-1/NF-21 complex is evident by the slight decrease in the mobility of the corresponding band (Figure 3B, lanes 4 and 6 and Figure S5A). Interestingly, NF-21-Alexa did not efficiently bind DOCTR-1 even in the absence of K-58A, as indicated by the absence of the red-labeled DOCTR-1 band (Figure 3A, lane 5). This data indicates that under experimental conditions (2 mM $MgCl_2$, 37 °C), DOCTR-1 did not tightly bind NF-21 from solution due to low affinity (melting temperatures of 35.7 and 35.8 °C for Dz-a and Dz-b, respectively). For the tight binding to DOCTR-1, NF-21 needed to be cut out from K-58A first, and then transfers it to closely located the Dz-a and Dz-b portion of the same DOCTR-1. In contrast, at 50 mM Mg^{2+} melting temperatures of Dz-a and Dz-b fragments with NF-21 increase to 43.1 °C and 42.8 °C, respectively, which led to the formation of DOCTR-1/NF-21-Alexa complex (Figure S5B).

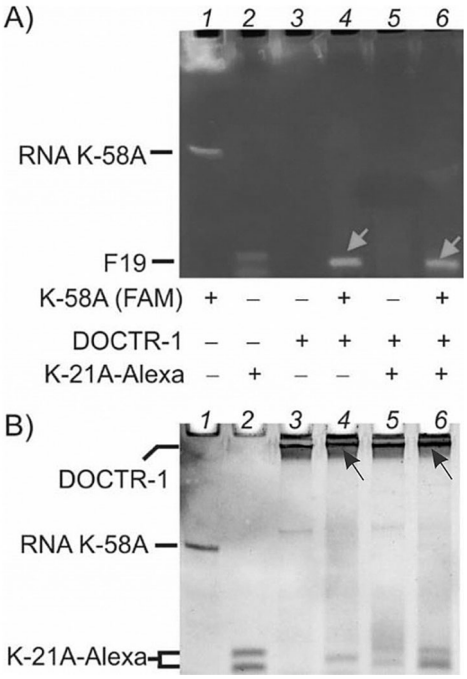

Figure 3. Once cut out from RNA K-58A, NF-21 does not exchange with the solution-residing NF-21-Alexa. DOCTR-1 (100 nM) was pre-incubated with 100 nM K-58A-FAM for 2 h followed by addition of 100 nM NF-21-Alexa (lane 6). K-58A or RNA NF-21-Alexa were incubated with DOCTR-1, lanes 4 and 5, respectively. Lanes 1, 2, and 3 contained RNA K-58A, RNA NF-21-Alexa or DOCTR-1 controls, respectively. After incubation 2 h at 37 °C, the reaction mixtures were separated in 10% native 2 mM Mg^{2+} polyacrylamide gel. A) Image obtained under UV light without staining. Arrow indicated F-19 cleavage product K-58A RNA. NF-21-Alexa migrated as a double band in all samples because of imperfection of chemical DNA synthesis. B) Same gel imaged after GelRed staining. Arrows indicate DOCTR-1/NF21 complex migrating slower than DOCTR-1 (for more convincing image see Figure S5A).

Transfer of the NF-21 fragment to Dz-a and Dz-b stabilizes the catalytic Dz core and thus activates DOCTR-1 actuating function. The actuating function response was first monitored by fluorescence, where Dz-a and Dz-b fluorogenic F sub (Figure 1B). Under this temperature, DOCTR-1 activated by either K-58A or NF-21A produced signal ≈2 times above the background. The low signal was due to suboptimal binding of F sub to the Dz-a and Dz-b. We opted to conduct further optimization using a housekeeping gene mRNA fragment rather than improving results with the model F sub. Neither addition of K-58G nor NF-21G triggered signal above the background (Figure 4A), thus proving high selectivity of DOCTR-1's actuating function.

In contrast, tile-free Dz-a and Dz-b failed to produce fluorescent response in 2 mM Mg^{2+}, but were able to respond in 50 mM Mg^{2+} (Figure S6A). The fluorescent responses of DOCTR version lacking Dz1 and Dz2 was almost identical to that of DOCTR-1 (Figure S6B) indicating that Dz1 and Dz2 did not interfere in the performance of actuating function.

Next, we adjusted DOCTR-1 for cleave of a housekeeping gene sequence. As a cleavage target, we selected PSMA3 gene coding for a subunit of 20S proteasomal core, which is

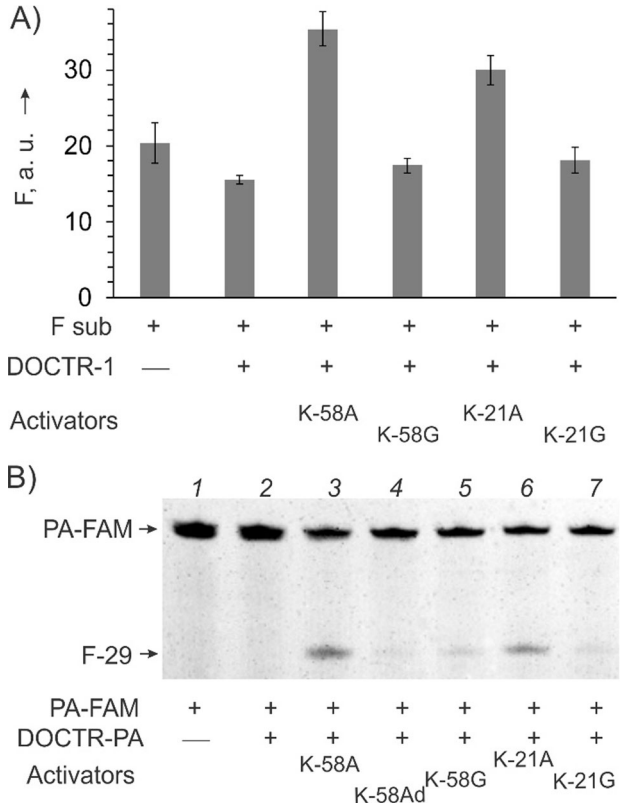

Figure 4. The performance of DOCTR's actuating function. A) DOCTR-1 produced a signal above the background only in the presence of fully matched K-58A and K-21A. Samples contained 200 nM F sub, 10 nM DOCTR-1, and 10 nM activators K-58A, K-58G, NF-21A or NF-21G as indicated. Fluorescent measurements were taken at 517 nm after 4 h incubation at 30°C in buffer 1. B) Actuating function of DOCTR-1 targeting mRNA fragment of the PSMA3 gene (PA). All lanes contained 500 nM PA-FAM (Table S1). Cleavage of PA-FAM by 100 nM DOCTR-PA in the presence of 100 nM activators K-58A, K-58G, NF-21A or NF-21G as indicated. Samples were analyzed in 12.5% PAG after 16 h of incubation at 37°C in buffer 1. The photograph was taken from an unstained gel.

essential for cell survival.[22] The target was represented by FAM-labeled fragment PA-FAM (Figure S7). Cleavage of PA-FAM by DOCTR-PA generated expected 29-nt fluorescently labeled fragment (F-29), upon activation by either K-58A or NF-21A (Figure 4B, lanes 3 and 6). No PA-FAM cleavage was observed in the presence of single base mismatched K-58G or NF-21G thus demonstrating excellent selectivity. Importantly, DOCTR-PA could not be activated by the uncleavable analog of K-58Ad (Figure 4B, lane 4), which further verifies the importance of cutting out the activator sequence NF-21 form the context of the long cancer marker sequence prior achieving activation of the actuating function.

In this work, we addressed some problems of DNA-based anti-cancer OGT agents by designing a multi-functional nanostructure that can accommodate several functional units acting in cooperation with each other. This study makes a conceptual step toward improving traditional anti-cancer OGT agents. Traditional OGT agents are designed to suppress cancer marker RNAs, which may or may not affect cancer cell viability. Indeed, if a marker is expressed only in cancer cells, it is not required for cell functioning. For example, some cancer cells bearing KRAS mutation retain viability even after KRAS knock down.[19] On the other hand, if a gene is expressed in all cells (overexpressed in cancer), suppression of this gene should inevitably affect normal cells. We and others, proposed to activate an OGT agent by a cancer marker followed by targeting another RNA, crucial for cell viability.[23] This approach promises both to increase efficiency and reduce side effects of the traditional OGT agents. Accordingly, DOCTR-1 was equipped with separate recognition and cleavage functions.

A fundamental problem of all hybridization-based approaches is their low selectivity under physiological conditions.[24] Split Dz probe can solve this problem.[21] DOCTR-1 equipped with split Dz construct was able to differentiate RNA differing by a single nucleotide under near physiological conditions. Importantly, in this study the least destabilizing G-T mismatch was differentiated from A-T base pair under near physiological conditions.

All functional strands were attached to a common DNA scaffold, which ensured cooperativity of all the components. For example, release of NF-21 was observed only by the tile-attached but not tile-free Dz1 and Dz2. Another evidence of cooperativity is the fact that Dz-a and Dz-b strands were active within DOCTR structure at 2 mM Mg^{2+} lost their activity in detached form.

DOCTR-1's recognition/processing unit (Dz1 and Dz2) cooperatively bind and unwind RNA marker secondary structure, while lose their affinity to the short cleavage product (NF-21) thus promoting its transfer to the neighboring Dza/Dzb actuating function. The complexity of this multi-catalytic system is comparable with that of enzymatic supramolecular assemblies, while accessibility via rational designed and custom oligonucleotide synthesis offers a hope for future outperforming enzyme-based OGT strategies by DNA nanomachines.

Conclusion

In conclusion, we have introduced a DNA nano-construct with recognition/processing and actuating functions. This device was able to selectively recognize an RNA sequence of mutated KRAS gene, process it by cutting out a fragment, and use the fragment to activate cleavage of another RNA. Both processing and actuating functions are highly selective, where only mutated sequence is cleaved or used as an activator. This development lays a foundation for the future anti-cancer drugs based on artificially designed nucleic acid nanostructures.

Acknowledgements

The authors are grateful to Dr. Gerasimova for useful discussion and corrections. This work was supported by UCF COS startup funds and by NSF SHF 1907824.

Conflict of interest

The authors declare no conflict of interest.

Keywords: deoxyribozymes · DNA nanotechnology · gene therapy · KRAS gene · split probes

[1] a) Y. Benenson, T. Paz-Elizur, R. Adar, E. Keinan, Z. Livneh, E. Shapiro, *Nature* **2001**, *414*, 430 – 434; b) I. Aprahamian, *ACS Cent. Sci.* **2020**, *6*, 347 – 358.

[2] H. Ramezani, H. Dietz, *Nat. Rev. Genet.* **2020**, *21*, 5 – 26.

[3] L. He, D. Q. Lu, H. Liang, S. Xie, C. Luo, M. Hu, L. Xu, X. Zhang, W. Tan, *ACS Nano* **2017**, *11*, 4060 – 4066.

[4] H. Peng, X. F. Li, H. Zhang, X. C. Le, *Nat. Commun.* **2017**, *8*, 14378.

[5] A. E. Prigodich, D. S. Seferos, M. D. Massich, D. A. Giljohann, B. C. Lane, C. A. Mirkin, *ACS Nano* **2009**, *3*, 2147 – 2152.

[6] Y. Lv, R. Hu, G. Zhu, X. Zhang, L. Mei, Q. Liu, L. Qiu, C. Wu, W. Tan, *Nat. Protoc.* **2015**, *10*, 1508 – 1524.

[7] S. Li, Q. Jiang, S. Liu, Y. Zhang, Y. Tian, C. Song, J. Wang, Y. Zou, G. J. Anderson, J. Y. Han, et al., *Nat. Biotechnol.* **2018**, *36*, 258 – 264.

[8] A. Ora, E. Jarvihaavisto, H. Zhang, et al., *Chem. Commun.* **2016**, *52*, 14161 – 14164.

[9] A. M. Quemener, L. Bachelot, A. Forestier, E. Donnou-Fournet, D. Gilot, M. D. Galibert, *Wiley Interdiscip. Rev. RNA* **2020**, https://doi.org/10.1002/wrna.1594.

[10] G. Palomino-Vizcaino, L. M. Alvarez-Salas, in *Nucleic Acid Nanotheranostics* (Eds. M. Filice and J. Ruiz-Cabello), Elsevier, **2019**, Chapter 1.

[11] C. C. Ma, Z. L. Wang, T. Xu, Z. Y. He, Y. Q. Wei, *Biotechnol. Adv.* **2020**, *40*, 107502.

[12] D. M. Kolpashchikov, *Acc. Chem. Res.* **2019**, *52*, 1949 – 1956.

[13] D. H. Burke, N. D. Ozerova, M. Nilsen-Hamilton, *Biochemistry* **2002**, *41*, 6588 – 6594.

[14] D. D. Nedorezova, A. F. Fakhardo, D. V. Nemirich, E. A. Bryushkova, D. M. Kolpashchikov, *Angew. Chem. Int. Ed.* **2019**, *58*, 4654 – 4658; *Angew. Chem.* **2019**, *131*, 4702 – 4706.

[15] S. K. Silverman, *Trends Biochem. Sci.* **2016**, *41*, 595 – 609.

[16] G. A. Hobbs, C. J. Der, K. L. Rossman, *J. Cell Sci.* **2016**, *129*, 1287 – 1292.

[17] S. H. Yu, T. H. Wang, L. C. Au, *Biochem. Biophys. Res. Commun.* **2009**, *378*, 230 – 234.

[18] T. Golan, E. Z. Khvalevsky, A. Hubert, et al., *Oncotarget* **2015**, *6*, 24560 – 24570.

[19] A. Singh, P. Greninger, D. Rhodes, L. Koopman, S. Violette, N. Bardeesy, J. Settleman, *Cancer Cell* **2009**, *15*, 489 – 500.

[20] S. W. Santoro, G. F. Joyce, *Biochemistry* **1998**, *37*, 13330 – 13342.

[21] a) D. M. Kolpashchikov, *ChemBioChem* **2007**, *8*, 2039 – 2042; b) E. Mokany, S. M. Bone, P. E. Young, T. B. Doan, A. V. Todd, *J. Am. Chem. Soc.* **2010**, *132*, 1051 – 1059; c) A. J. Cox, H. N. Bengtson, K. H. Rohde, D. M. Kolpashchikov, *Chem. Commun.* **2016**, *52*, 14318 – 14321; d) A. L. Smith, D. M. Kolpashchikov, *ChemistrySelect* **2017**, *2*, 5427 – 5431.

[22] O. Coux, K. Tanaka, A. L. Goldberg, *Annu. Rev. Biochem.* **1996**, *65*, 801 – 847.

[23] D. D. Nedorezova, A. F. Fakhardo, T. A. Molden, D. M. Kolpashchikov, *ChemBioChem* **2020**, *21*, 607 – 611.

[24] D. M. Kolpashchikov, *Chem. Rev.* **2010**, *110*, 4709 – 4723.

Manuscript received: May 2, 2020
Revised manuscript received: June 21, 2020
Accepted manuscript online: July 20, 2020
Version of record online: ■■ ■■, ■■■■

Research Articles

DNA Nanotechnology

T. A. Molden, C. T. Niccum,
D. M. Kolpashchikov* ——— ▮▮▮▮–▮▮▮▮

Cut and Paste for Cancer Treatment: A DNA Nanodevice that Cuts Out an RNA Marker Sequence to Activate a Therapeutic Function

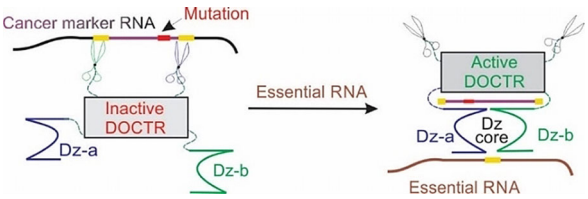

A DNA nanoconstruct, named DOCTR, selectively recognizes a mutant RNA sequence that is a marker for cancer. The nanodevice then cuts out a fragment (purple) and uses this fragment to activate the cleaving function, which damages another RNA essential for cancer cell survival.